Istraživanja i projektovanja za privredu
ISSN 1451-4117
DOI:10.5937/jaes0-39911
www.engineeringscience.rs

iipp publishing

Journal of Applied Engineering Science
Vol. 21, No. 1, 2023
Original Scientific Paper
Paper number: 21(2023)1, 1066, 212-223

DEVELOPMENT OF WIND-SOLAR MAPS IN AQABA, JORDAN AS POTENTIAL SOURCES FOR POWER GENERATION

Mohanad Al-Ghriybah[1]*, Djamal Hissein Didane[2]

[1] Department of Renewable Energy Engineering, Faculty of Engineering, Isra University, Amman-Jordan
[2] Center for Energy and Industrial Environment Studies, Universiti Tun Hussein Onn Malaysia, Malaysia
** mohanad.alghriybah@iu.edu.jo*

The potential for free, clean, and limitless energy from renewable sources has long been recognized. However, because of a lack of thorough wind and solar maps, expertise, and public understanding of the significance of these resources in the country, Jordan continues to rely on non-renewable sources for its energy needs. The main objective of this study is to analyze the potential of solar and wind energies as renewable resources for power generation. Weibull distribution function with two parameters and the Angstrom-Prescott model, respectively, are used in this study to offer estimates of the wind and solar energy in the coastal city of Jordan, Aqaba during a five-year period. According to the assessment of wind potential, the annual means of the shape and scale parameters at 10 m for the studied station varied between (1.65 to 1.73) and (4.42 to 4.86), respectively. During the dry season, the wind speed was seen to be stronger, while during the wet season, it was seen to be slower. The maximum power density is found to be in September with values of 622.81 W/m2 and 192.74 W/m2 for the elevations 80 m and 10 m, respectively. According to the forecast for solar potential in this area, the city's global solar radiation is promising for the production of solar energy. The maximum global solar radiation is found to be 8.3 KWh/m2 in June. Results also demonstrated that Aqaba city is suitable for wind and solar power generation.

Keywords: wind assessment, solar assessment, Jordan, angstrom-prescott, weibull distribution

1 INTRODUCTION

The main factor in a country's development is energy. The globe is undergoing an economic and technological revolution, which is causing an abrupt rise in energy demand [1]. Technology breakthroughs are made possible by energy, but there are also drawbacks that must be considered. Fossil fuels can harm the planet in a number of ways, with pollution and global warming being two major examples [2]. Energy alternatives have emerged as awareness of energy consumption increases. However, given the rising demand for energy, it is now vital to research different energy sources like wind and solar. For instance, the availability of wind energy varies according to a number of factors, such as the elevation of the land above sea level and the environment, where the wind may not reach the turbine sufficiently [3]. About 10 million MW of energy may be produced by wind energy, which would be sufficient to replace the utilization of fossil fuels [4]. Utilizing wind turbines with suitable designs would allow for the harvesting of such potentials [5]. Solar energy can also be used to generate electricity for a number of different purposes. Contrary to conventional energy sources, solar energy (photovoltaic, solar thermal, and solar power) has major environmental advantages that support the sustainable advancement of human endeavors [6]. Numerous benefits of solar energy technology include lowering greenhouse gas emissions, reducing the need for power grid transmission lines, and improving the quality of water supplies [7].

Although the area is typically quite dry, Jordan's climate can range from a more Mediterranean environment to a desert climate [8]. The desert regions see winter temperatures of 19 to 22 °C, while the southern and northern highlands experience temperatures between 9 and 13 °C. Summertime temperatures in the Jordanian Valley range from 38 to 39 °C, whereas they are between 26 and 29 °C in the desert [9]. Wintertime sees the most precipitation, at 75%. The Dry Sirocco (Khamsin) winds, which can cause significant temperature anomalies with increases of up to 15°C, have an impact on Jordan's climate. The northern winds, which originate in the north and northeast and raise daytime temperatures, are another contributing factor [10]. Even so, the climates of rural and coastal places might change due to differences in altitude and temperature swings, which can alter wind and solar energy [11]. The Hashemite Kingdom of Jordan's economy is under tremendous pressure due to rapid population growth [12]. Finding new sources of economic growth is necessary, as are long-term advantages for the region's 10.6 million citizens today and future generations. Although the COVID-19 health issue has made Jordan's economic difficulties much worse, the nation is determined to advance the use of domestic energy resources [13]. Jordan became a leader in the area of renewable energy as the percentage of electricity generated from renewable sources increased from 13 percent in 2019 to over 26 percent in 2021 [14]. The nation has put in place essential laws and policies to encourage the growth of renewable energy sources, such as solar photovoltaic (PV) and onshore wind. A sustainable future energy supply, diversification of the country's energy mix, a greater reliance on local energy resources, improved energy security, and decreased energy dependence and electricity supply costs are all recommended in the updated Master Strategy for the Energy Sector 2020–2030. By 2030, the policy aims to have renewables account for 14% of the entire energy mix and 31% of all power production capacity [15].

A method known as Weibull distribution can be employed to provide a clear image of the available potentials due to the complexity of the data available for calculating the potentiality of wind energy [16]. In order to determine the

frequency and density of wind speed circulation, the statistical two-parameter distribution method is frequently utilized. On the other hand, because of its simplicity and validity, the Angstrom-Prescott methodology is the most often used method for solar assessment. Several studies have been conducted using the Weibull distribution. Research accomplished by Mondal et al., [17] in Bangladesh showed that the country has a promising wind potential for electricity generation with a maximum wind power density of about 120 w/m2 in the Chittagong division. Another study by Shoib et al., [18] has been conducted for assessing wind potential in Malaysia. Results concluded that the maximum wind power density is found to be in Melaka with a value of 26 W/m2. Iranian meteorological data from 14 provinces and 30 sites dispersed throughout the country were used to analyze the performance of the researched approaches. Results showed that, in terms of mistakes, the empirical method is preferable to the technique under investigation [19]. Medina's wind energy potential was evaluated using the Weibull probability distribution [20]. Important discoveries included a 2.9 m/s wind speed recurrence with a probability of about 30%. Hassane et al. [21] used the statistical two-parameter Weibull distribution function and the Angstrom-Prescott model, respectively, to conduct assessments of both wind and solar energy in the Sahelian zone in Chad during a ten-year period. Results showed that the wind power density in the region was up to 220 w/m2. Alami et al., [22] examined the relationship between solar irradiance and the number of hours with sunshine in Sharjah, United Arab Emirates. Results showed that the model predicted the solar potential in the city with an accurate form. According to the study conducted by Serban et al., [23] Romania's wind potential falls into the category of "good". In a different investigation, wind speed power density and frequency distribution were computed using the Weibull distribution in nine different locations in Jordan [24]. Results showed that Irbid has the lowest wind power density, followed by Ghor Al Safi, and King Hussein Airport has the highest, followed by Queen Alia Airport. Another study showed that the capital city of Jordan, Amman has a wind power density of about 48 w/m2 [25]. Recently, a study by Al-Ghriybah et al.,[26] showed that Ajloun, Jordan is suitable for small-scale wind turbines based on the wind levels in the city.

Coastal regions is preferable for power generation due to the conditions that available in such regions such as the pressure difference between the land and the sea which creates a high pressure difference and as a result a high wind speed. Throughout the literature, there is no specific study that assesses the wind and solar energies in the only coastal city of Jordan, Aqaba. Additionally, most of the available studies have assessed the wind potential at 10 m recorded wind speed. Which is not accurate enough due to the large heights of the wind turbine tower. Based on that, this study aims to assess wind and solar potential in the coastal city of Aqaba based on five years of collected data. Moreover, this study aims to evaluate the wind potential at different heights (10 m and 80 m) which will provide a more accurate assessment for wind applications.

2 SITE DESCRIPTION

Aqaba (29.5321° N, 35.0063° E) is Jordan's only coastal city, as well as the biggest and most populated city on the Gulf of Aqaba. It is located in the south of Jordan with an overall area of 375 km2 (Fig. 1). Aqaba city has a population of about 217,900 widespread in two main districts (Aqaba Qasabah District with a population of 184,150 and Quairah District with a population of 33,750). Its borders with Saudi Arabia, occupied Palestine, and the Gulf of Aqaba from the west, east, and south, respectively. July is the warmest month in Aqaba with a daily average temperature of 36.8°C whereas at night the temperature is typically lower with a value of 22.7°C. The average sunny hours in the city is about 11.4 hours.

Fig. 1. Map of Aqaba, Jordan

3 METHODS, THEORETICAL, AND MATHEMATICAL MODELS

The relevant meteorological data were gathered, and then they were statistically analyzed to determine the average mean wind speed, temperature, and sky condition. The data that have been analyzed are then employed in other equations that calculate the quantity of available power to be used by evaluating wind and solar resources.

3.1 Wind energy assessment

Several considerations must be made before the wind energy potential calculation can be made. These include figuring out the wind density and how much energy the wind generates. To estimate a site's wind potential, a variety of assessment methods are employed. The Weibull distribution is the assessment method that is most frequently utilized. The wind variations at a certain location can be represented by this distribution. The following is a representation of this function's mathematical model [27]:

$$F(v) = (k/c)(v/c)^{k-1} \exp[-(v/c)^k] \quad (1)$$

The quantity F(v) in this equation represents the probability density at a specific wind speed. While k and c, respectively, are a stand-in for the shape and scale parameters. The wind potential in a certain location might be described using shape and scale parameters. The shape parameter, k, is a measure of the breadth of the wind distribution, while the scale parameter, c, specifies the site's wind availability. Shape and scale parameters are expressed as follows [28]:

$$k = \sqrt{0.6889 v_{ave}} \quad (2)$$

$$c = \frac{v_{ave}}{\Gamma(\frac{k}{k} + \frac{1}{k})} \quad (3)$$

The average wind speed is denoted by the symbol v_{ave} in this equation, whereas the gamma function is denoted by the symbol Γ.

The mass of air in the Earth's atmosphere has an impact on the wind, which is a source of kinetic energy. The mass of the air in relation to its volume, or air density, affects wind power density. It can also be calculated by dividing the wind's cross-sectional area by its speed. The following equation can be used to measure wind power density.

$$P = 0.5 \rho_{air} U^3 A \quad (4)$$

Where $\rho_{air} = 1.225\ kg/m^3$ and it represents air density, U represents prevailing wind speed, and A represents swept area of the used turbine. However, the wind power density can be estimated using an equation in the Weibull distribution function as follows [29]:

$$\frac{P}{A} = \int_0^\infty 0.5 \rho_{air} v^3 f(v) dv = 0.5 \rho_{air} c^3 \Gamma\left(1 + \frac{3}{k}\right) \quad (5)$$

It is desirable to determine which wind speed has the most energy carried (V_{maxE}) and which speed is the most probable (V_{mp}) since wind speed and carried energy vary with each other. This can be done using the following equation [30]:

$$V_{max,E} = c\left(\frac{k}{k} + \frac{2}{k}\right)^{K^{-1}} \ (m/s) \quad (6)$$

$$V_{mp} = c\left(\frac{k}{k} - \frac{1}{k}\right)^{k^{-1}} \ (m/s) \quad (7)$$

3.2 Solar energy assessment

Due to the different factors that affect how solar radiation is attenuated, the Sun encounters incidents and diffuses solar radiation. These consist of dust and water vapor. The total of the incident and diffuse radiation represents the solar flux at the surface of the globe. Accordingly, global solar radiation (H_g) and can be represented by the following equation [31]:

$$H_g = H_0 K_T \quad (8)$$

Where on a horizontal surface, H_0 is the solar radiation from space and it is not reliant on any other geographic factors; it just depends on latitude. K_T represents the clearness index (a measure of the clearness of the atmosphere). However, because of attenuation, H_g is greatly influenced by where it is on the earth's surface, and its value is lower than that of extraterrestrial irradiation and H_0. Angstrom was the leader in solar radiation modeling (1924). He created a linear model for predicting the ratio of solar radiation (Sa/Sm) using sunlight data gathered from meteorological stations of a site, where Sa is the average daily sunshine duration and Sm is the maximum of the average monthly

duration of sunshine on the site. After that, this model was enhanced by Prescott in 1940 and Page in 1961 by accounting for Ho and the length of the sunny days in the relation given below [32].

$$\frac{H_g}{H_0} = C_1 + C_2\left(\frac{S_a}{S_m}\right) \tag{9}$$

Where H_0, C_1, C_2, and Sa can be estimated using the following equations [33]:

$$H_0 = I_{Sc}\left[7.64 + 2.52\cos\left(\frac{360}{365}D_y\right)\right] * \left[\sin(\omega_s)\cos(L)\cos(\delta) + \frac{2\pi\omega_s}{360}\sin(\delta)\sin(l)\right] \tag{10}$$

$$C_1 = 0.323\left(\frac{S_a}{S_m}\right) + 0.235\cos(L) - 0.11 \tag{11}$$

$$C_2 = -0.694\left(\frac{S_a}{S_m}\right) - 0.533\cos(L) + 1.449 \tag{12}$$

$$S_m = \frac{24 * \cos^{-1}(-\tan(\delta)\tan(l))}{\pi} \tag{13}$$

Where I_{Sc}= 1367 w/m^2, D_y represents the total days in one year, ω_s is the angle of the sunset hour and it can be calculated using Eq.13, L is the latitude, and δ is the solar declination angle and it can be estimated using Eq.14 [34].

$$\omega_s = \frac{\pi * S_m}{24} \tag{14}$$

$$\delta = 23.45 * \sin\left(280.1 + 0.986D_y\right) \tag{15}$$

4 RESULTS AND DISCUSSION

To provide the reader with a sense of consistency and clarity, the results are presented in two different portions. The wind energy evaluation for the Jordanian seaside city of Aqaba is presented in the first section, while the solar energy assessment is covered in the second. At two distinct heights, 10 m and 80 m, the evaluation of wind resources was examined.

4.1 Wind analysis results

4.1.1 Variation in Monthly Wind Speed

The annual average wind speed in Aqaba varies from 4.6 to 6.5 m/s at 80 m above sea level and from 2.5 to 5.4 m/s at 10 m. Fig. 2 illustrates the variation in wind speed for the years from 2016 to 2020 at 10 m height. It can be seen from the plot that wind speed data for the various months are following the same trend with a little variation between different years. The maximum wind speed can be noticed in September whereas the lowest value can be found in December. This variation can be attributed to the uneven solar radiation that reaches the city with different values each year. This variation creates different pressure gradients and so on different wind speeds. Moreover, Fig. 3 shows a comparison between the averaged wind speed at 10 m and 80 m heights. It can be seen from the figure that the maximum wind speed was 8.56 at 80 m and 5.40 at 10 m in September. This shows that the wind speed increases with the increase of height and this is due to the phenomenon called wind shear. However, both the evaluation of wind resources and the design of wind turbines are influenced by wind shear. In terms of seasonal variance, the summer season, which runs from June to September, always has the highest wind speeds. The precipitation rate always approaches zero millimeters during this season, when it is at its lowest. This demonstrates an inverse relationship between the rate of precipitation and wind speed, meaning that the greater the average wind speed, the lower the rate of precipitation.

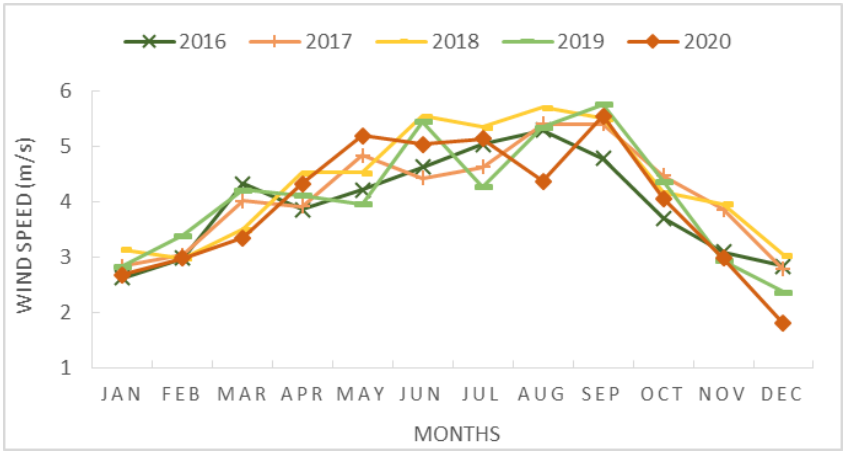

Fig. 2. Monthly variation in wind speed during 5 years

Fig. 3. Averaged wind speed variations at different heights

4.1.2 Power and energy in Aqaba's wind

The prevailing wind speed, the wind carrying max energy, wind most probable, energy, and power densities were estimated at the desired locations by using the two parameters Weibull distribution. Table 1 shows the annual results of the energy and power assessment at two different heights (10m and 80m). It can be seen from the table that the highest wind speed was in the year 2018 with values of 4.32 at 10 m elevation and 7.11 at 80 m elevation. On the other hand, the maximum power and energy densities were found in the same year with values of 111 W/m^2 and 978.8 KWh/m^2, respectively for the 10 m elevation and 383.87 W/m^2 and 3362.75 KWh/m^2, respectively for the 80 m elevation. These results are logical since the wind power and wind energy are proportional to the cube of the wind velocity. Additionally, it can be observed that the wind speed that carries maximum energy is about 7.58 and 10.7 at 10 m and 80 m elevations, respectively. Moreover, the values of the most probable wind speed were 2.94 for 10 m elevation and 6.12 for 80 m elevation.

Table 1. Annual power and energy at different heights

Year	2016	2017	2018	2019	2020
At 10 m elevation					
$v_{ave}\ (m/s)$	3.94	4.13	4.32	4.08	3.95
$V_{max,E}\ (m/s)$	7.14	7.35	7.58	7.30	7.15
$V_{mp}\ (m/s)$	2.50	2.71	2.94	2.66	2.51
$P/A\ (W/m^2)$	89.8	100	111	97.3	90.2
$E/A\ (KWh/m^2)$	786.8	876.1	978.8	852.7	790.8
At 80 m elevation					
$v_{ave}\ (m/s)$	6.60	6.85	7.11	6.78	6.59
$V_{max,E}\ (m/s)$	10.1	10.4	10.7	10.3	10.1
$V_{mp}\ (m/s)$	5.54	5.83	6.12	5.74	5.53

Year	2016	2017	2018	2019	2020
$P/A\ (W/m^2)$	316.79	348.67	383.87	339.13	315.85
$E/A\ (KWh/m^2)$	2775.09	3054.34	3362.75	2970.81	2766.85

The monthly wind power and energy densities are illustrated in Fig.4 for 10 m and 80 m elevations. It can be observed from the figure that the maximum power and energy densities can be found in September with values of 622.81 W/m^2 and 192.74 W/m^2 for the elevations 80 m and 10 m, respectively. On the other hand, it can be observed that the lowest power and energy densities can be found in December. This is due to the seasonal changes where it can be noticed that the summer season has the highest power density and the winter season has the lowest power density. Furthermore, it was found that extrapolating the wind data from 10 m to 80 m height increased the wind speed by approximately 67%, leading to an increase in power potential of almost 245%.

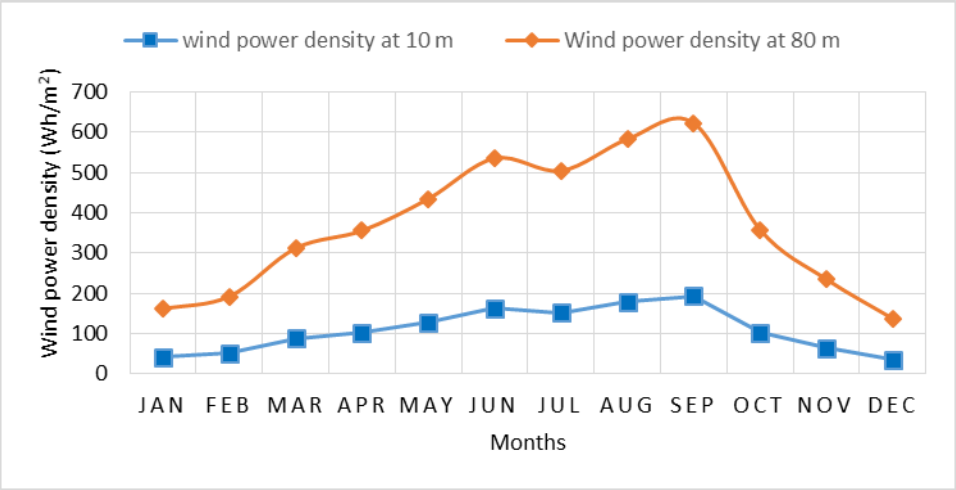

Fig. 4. Wind power density at 10 m and 80 m elevations

4.1.3 Weibull distribution parameters

The Monthly and the annual shape and scale parameters of Weibull distribution (k and c) for the city under study for 5 years are shown in Table 2 and Table 3 for both 10 m and 80 m elevations, respectively. It was noted that over the examined years, the value of k varied between 1.11 and 1.99 at 10 m of height and between 1.55 and 2.49 at 80 m of height. Given that a stable and persistent site typically has a shape parameter value in the 1.5 to 3 range, commencing at a height of 10 m above the ground, the Aqaba site might be regarded as stable for the majority of the year (aside from January, February, November, and December). At an altitude of 80 meters, however, it is evident that all of the months can be categorized as stable for the production of wind energy. According to Table 3, it can be seen that the annual shape parameter is in the range of 1.65 to 1.73 at 10 m height and in the range of 2.13 to 2.21 at 80 m height. However, this indicates that the annual shape parameter thought the years is almost the same and has a slight change. Greater temporal changes were seen in the scale parameter, c. The largest scale parameter, measuring 6.50 m/s at 10 m and 10.17 m/s at 80 m, was recorded in September 2019. On the other hand, the lowest value of the scale parameter was noticed to be in December 2020 with a value of 1.87 m/s at 10 m height and 3.88 at 80 m height. The annual values of c were in the range of 4.42 to 4.86 at 10 m and 7.45 to 8.05 at 80 m. This amply demonstrates both the large variance in wind with altitude and the enormous variation in wind strength in Aqaba over the course of the different months and years.

Table 2. Monthly k and c

		Year of 2016		Year of 2017		Year of 2018		Year of 2019		Year of 2020	
Month	Parameters	10 m	80 m	10 m	80 m	10 m	80 m	10 m	80 m	10 m	80 m
Jan	V_{ave}	2.62	4.75	2.83	5.05	3.14	5.49	2.83	5.04	2.67	4.82
	k	1.34	1.81	1.40	1.86	1.47	1.95	1.40	1.86	1.36	1.82
	c	2.86	5.34	3.10	5.69	3.47	6.20	3.10	5.69	2.92	5.42
Feb	V_{ave}	2.98	5.27	3.04	5.35	2.98	5.27	3.40	5.86	2.98	5.27
	k	1.43	1.91	1.45	1.92	1.43	1.91	1.53	2.01	1.43	1.91
	c	3.29	5.94	3.35	6.03	3.29	5.94	3.77	6.61	3.29	5.94
Mar	V_{ave}	4.32	7.14	4.01	6.72	3.50	6.00	4.22	6.99	3.34	5.79
	k	1.73	2.22	1.66	2.15	1.55	2.03	1.70	2.20	1.52	2.00

		Year of 2016		Year of 2017		Year of 2018		Year of 2019		Year of 2020	
Month	Parameters	10 m	80 m	10 m	80 m	10 m	80 m	10 m	80 m	10 m	80 m
	c	4.85	8.06	4.49	7.58	3.89	6.78	4.73	7.90	3.71	6.52
Apr	v_{ave}	3.86	6.50	3.91	6.58	4.53	7.41	4.12	6.86	4.32	7.14
	k	1.63	2.12	1.64	2.13	1.77	2.26	1.68	2.17	1.73	2.22
	c	4.31	7.34	4.37	7.42	5.09	8.37	4.61	7.74	4.85	8.05
May	v_{ave}	4.22	6.99	4.84	7.82	4.53	7.41	3.96	6.65	5.19	8.30
	k	1.70	2.20	1.83	2.32	1.77	2.26	1.65	2.14	1.89	2.40
	c	4.73	7.90	5.44	8.83	5.09	8.37	4.43	7.50	5.85	9.35
Jun	v_{ave}	4.63	7.55	4.42	7.27	5.56	8.76	5.45	8.63	5.04	8.09
	k	1.79	2.28	1.75	2.24	1.96	2.46	1.94	2.44	1.86	2.36
	c	5.20	8.52	4.97	8.21	6.27	9.88	6.15	9.73	5.68	9.13
Jul	v_{ave}	5.04	8.09	4.63	7.55	5.35	8.49	4.27	7.07	5.14	8.23
	k	1.86	2.36	1.79	2.28	1.92	2.42	1.71	2.21	1.88	2.38
	c	5.68	9.13	5.20	8.52	6.03	9.58	4.79	7.97	5.79	9.28
Aug	v_{ave}	5.30	8.43	5.40	8.56	5.71	8.96	5.35	8.50	4.37	7.21
	k	1.91	2.41	1.93	2.43	1.98	2.48	1.92	2.42	1.74	2.23
	c	5.97	9.51	6.09	9.66	6.44	10.10	6.03	9.58	4.91	8.13
Sep	v_{ave}	4.78	7.75	5.40	8.56	5.50	8.69	5.76	9.03	5.56	8.76
	k	1.82	2.31	1.93	2.43	1.95	2.45	1.99	2.49	1.96	2.46
	c	5.38	8.75	6.09	9.66	6.21	9.81	6.50	10.17	6.27	9.87
Oct	v_{ave}	3.70	6.29	4.48	7.34	4.17	6.92	4.37	7.21	4.06	6.79
	k	1.60	2.08	1.76	2.25	1.69	2.18	1.74	2.23	1.67	2.16
	c	4.13	7.10	5.03	8.29	4.67	7.82	4.91	8.13	4.55	7.66
Nov	v_{ave}	3.09	5.42	3.86	6.50	3.96	6.64	2.93	5.20	2.98	5.27
	k	1.46	1.93	1.63	2.12	1.65	2.14	1.42	1.90	1.43	1.91
	c	3.41	6.11	4.31	7.34	4.43	7.50	3.22	5.85	3.29	5.94
Dec	v_{ave}	2.83	5.04	2.78	4.97	3.04	5.35	2.37	4.36	1.80	3.49
	k	1.40	1.86	1.38	1.85	1.45	1.92	1.28	1.73	1.11	1.55
	c	3.10	5.68	3.04	5.60	3.35	6.03	2.55	4.89	1.87	3.88

Table 3. Annual k and c

Year	2016	2017	2018	2019	2020
At 10 m elevation					
v_{ave}	3.94	4.13	4.32	4.08	3.95
k	1.65	1.69	1.73	1.68	1.65
c	4.42	4.63	4.86	4.57	4.43
At 80 m elevation					
v_{ave}	6.60	6.85	7.11	6.78	6.59
k	2.13	2.17	2.21	2.16	2.13
c	7.46	7.74	8.04	7.66	7.45

Figs. 5 – 7 and Figs. 8 – 10, respectively show the frequency distribution at 10 m and 80 m heights. These frequencies are able to predict the potential energy that the site's conversion system will produce. The three chosen years at a height of 10 m were found to have the same frequency pattern. However, the most frequent speed was between 1 m/s and 6 m/s during all studied years at 10 m height. On the other hand, wind frequency at 80 m was following a different trend than the 10 m height where the frequency of high velocities was more than the low velocities. The most frequent wind speed was between 3 m/s and 10 m/s during all studied years at 80 m height. However, it can be noticed that the frequency distribution decreases as the elevation increases and cover more strong wind speed but with lower frequency.

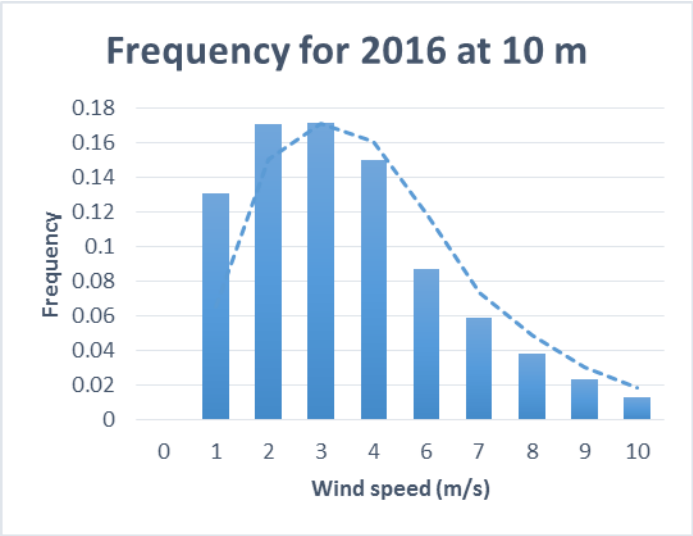

Fig. 5. Frequency at 10 m for the year 2016

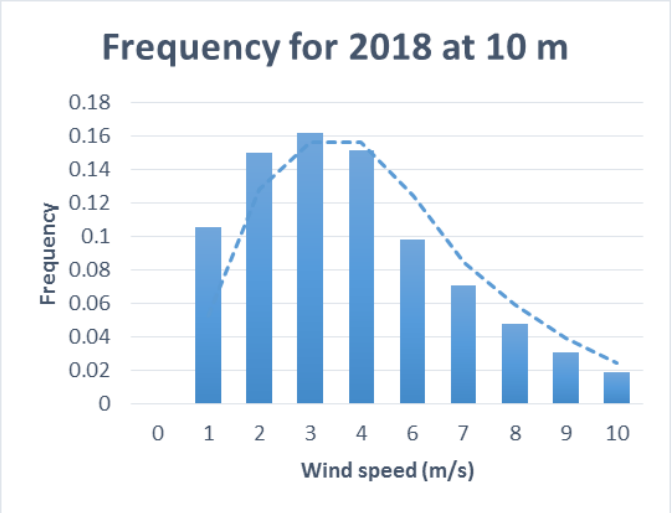

Fig. 6. Frequency at 10 m for the year 2018

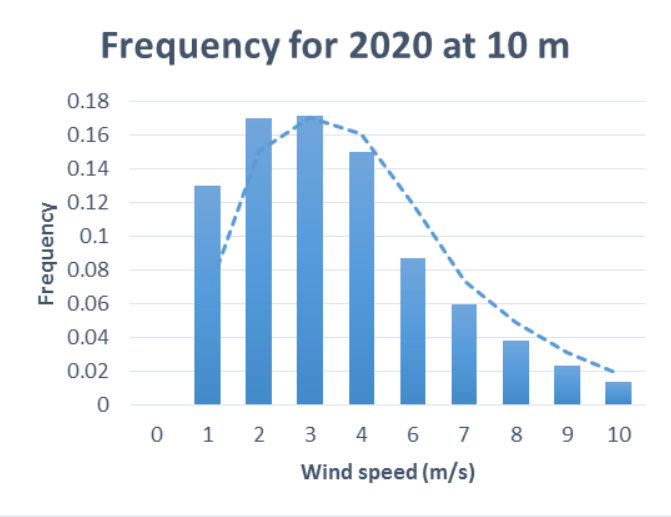

Fig. 7. Frequency at 10 m for the year 2020

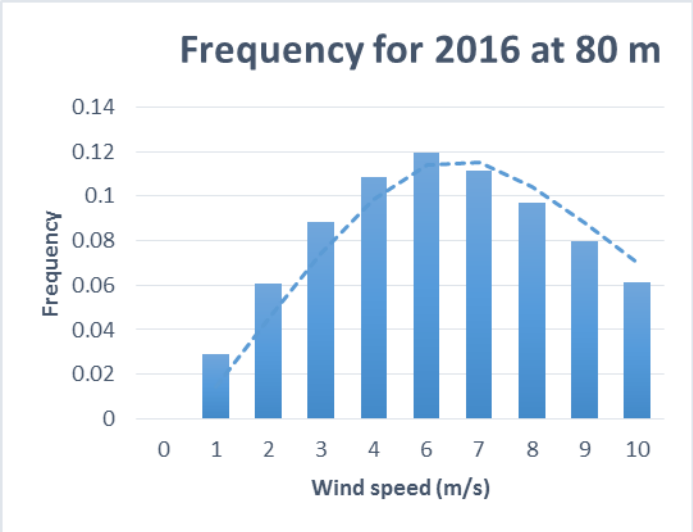

Fig. 8. Frequency at 80 m for the year 2016

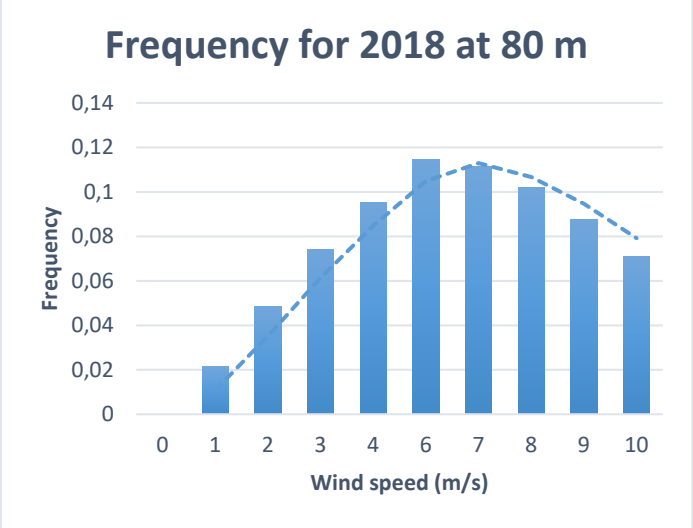

Fig. 9. Frequency at 80 m for the year 2018

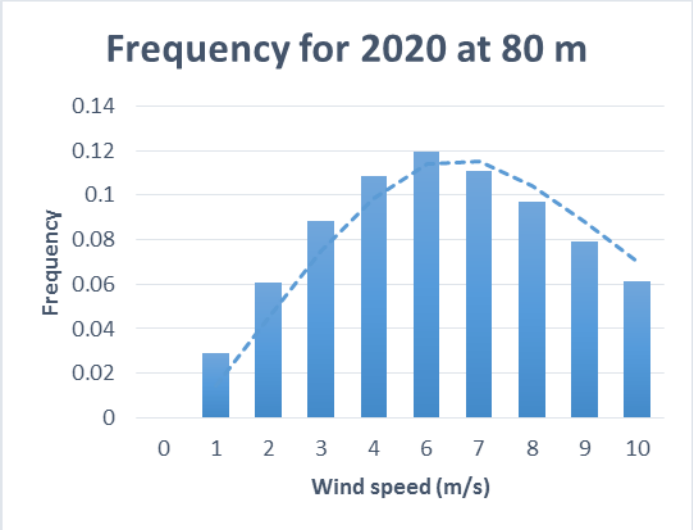

Fig. 10. Frequency at 80 m for the year 2020.

4.2 Solar analysis results

The global solar radiation parameters determined by the Angstrom model are presented in this section. The data were gathered over a five-year period. The equations for the model were used to determine all the parameters, and Fig. 11 illustrated the global solar radiation. It can be seen from the figure that the global solar radiation varies from 3.2 KWh/m^2 and 8.3 KWh/m^2. The lowest value can be found in December whereas the highest value can be found in June. Additionally, May, June, and July have a very close amount of radiation with values between 8.15 KWh/m^2

and 8.3 KWh/m^2. Low solar radiation can be found in the months October, November, December, and January. These values reflect that Aqaba city is suitable for solar power generation.

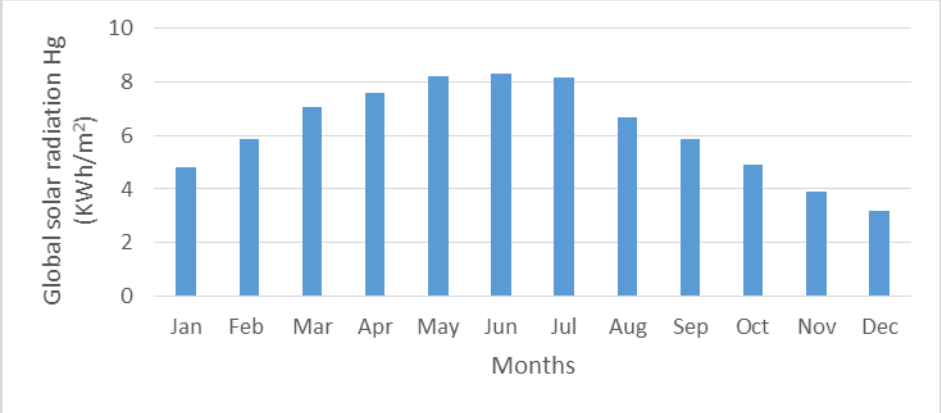

Fig. 11. Averaged monthly global solar radiation for Aqaba city

5 CONCLUSIONS

In this study, five-year metrological data for the coastal city of Jordan, Aqaba has been analyzed for both wind and solar energies using statistical methods. The main objective of the current work was to examine the potential for solar and wind energy and to conduct the first thorough analysis of these sources in the city of Aqaba. The wind energy potential and solar energy potential have been calculated using the Weibull density function and empirical Angstrom model, respectively. According to the assessment of wind potential, the annual means of the shape and scale parameters at 10 m for the studied station varied between (1.65 to 1.73) and (4.42 to 4.86), respectively. At the normal height of 10 meters, the annual mean wind speed in the city ranges from 2.5 m/s to 5.4 m/s, and the associated mean power density is between 35.47 W/m^2 and 192.74 W/m^2. According to Angstrom, the mean global solar radiation value is observed to be 8.3 KWh/m^2/day during June. This study reveals that Aqaba city is suitable for power generation from both solar and wind energies.

6 ACKNOWLEDGEMENTS

Communication of this research is made possible through monetary assistance by Universiti Tun Hussein Onn Malaysia and the UTHM Publisher's Office via Publication Fund E15216.

7 REFERENCES

[1] ZOU, C., MA, F., PAN, S., LIN, M., ZHANG, G., XIONG, B., YANG, Z. (2022). Earth energy evolution, human development and carbon neutral strategy. Petroleum Exploration and Development, 49(2), 468–488. https://doi.org/10.1016/S1876-3804(22)60040-5.

[2] Al-Ghriybah, M., Zulkafli, M. F., Didane, D. H., & Mohd, S. (2020). Performance of Double Blade Savonius Rotor at Low Rotational Speed. Journal of Computational and Theoretical Nanoscience, 17(2), 729–735. https://doi.org/10.1166/jctn.2020.8711.

[3] Al-Ghriybah, M., Zulkafli, M. F., & Didane, D. H. (2020). Numerical Investigation of Inner Blade Effects on the Conventional Savonius Rotor with External Overlap. Journal of Sustainable Development of Energy, Water and Environment Systems, 8(3), 561–576. https://doi.org/10.13044/j.sdewes.d7.0292.

[4] Trypolska, G., Kurbatova, T., Prokopenko, O., Howaniec, H., & Klapkiv, Y. (2022). Wind and Solar Power Plant End-of-Life Equipment: Prospects for Management in Ukraine. Energies, 15(5), 1662. https://doi.org/10.3390/en15051662

[5] Al-Ghriybah, M. (2022). Performance Analysis of a Modified Savonius Rotor Using a Variable Blade Thickness. EVERGREEN Joint Journal of Novel Carbon Resource Sciences & Green Asia Strategy, 9(3).

[6] Kou, G., Yüksel, S., & Dinçer, H. (2022). Inventive problem-solving map of innovative carbon emission strategies for solar energy-based transportation investment projects. Applied Energy, 311, 118680. https://doi.org/10.1016/j.apenergy.2022.118680.

[7] Li, G., Li, M., Taylor, R., Hao, Y., Besagni, G., & Markides, C. N. (2022). Solar energy utilisation: Current status and roll-out potential. Applied Thermal Engineering, 209, 118285. https://doi.org/10.1016/j.applthermaleng.2022.118285.

[8] Zittis, G., Almazroui, M., Alpert, P., Ciais, P., Cramer, W., Dahdal, Y., … Lelieveld, J. (2022). Climate Change and Weather Extremes in the Eastern Mediterranean and Middle East. Reviews of Geophysics, 60(3). https://doi.org/10.1029/2021RG000762.

[9] Monna, S., Abdallah, R., Juaidi, A., Albatayneh, A., Zapata-Sierra, A. J., & Manzano-Agugliaro, F. (2022). Potential Electricity Production by Installing Photovoltaic Systems on the Rooftops of Residential Buildings in

Jordan: An Approach to Climate Change Mitigation. Energies, 15(2), 496. https://doi.org/10.3390/en15020496.

[10] Al-Ghazawi, Z., & Alawneh, R. (2021). Use of artificial neural network for predicting effluent quality parameters and enabling wastewater reuse for climate change resilience – A case from Jordan. Journal of Water Process Engineering, 44, 102423. https://doi.org/10.1016/j.jwpe.2021.102423.

[11] Farrar, L. W., Bahaj, A. S., James, P., Anwar, A., & Amdar, N. (2022). Floating solar PV to reduce water evaporation in water stressed regions and powering water pumping: Case study Jordan. Energy Conversion and Management, 260, 115598. https://doi.org/10.1016/j.enconman.2022.115598.

[12] Breulmann, M., Khurelbaatar, G., Sanne, M., van Afferden, M., Subah, A., & Müller, R. A. (2022). Integrated Wastewater Management for the Protection of Vulnerable Water Resources in the North of Jordan. Sustainability, 14(6), 3574. https://doi.org/10.3390/su14063574.

[13] Khatatbeh, M., Khasawneh, A., Hussein, H., Altahat, O., & Alhalaiqa, F. (2021). Psychological Impact of COVID-19 Pandemic Among the General Population in Jordan. Frontiers in Psychiatry, 12. https://doi.org/10.3389/fpsyt.2021.618993.

[14] Alrwashdeh, S. S. (2022). Energy sources assessment in Jordan. Results in Engineering, 13, 100329. https://doi.org/10.1016/j.rineng.2021.100329.

[15] IRENA. (2021). Renewable Readiness Assessment: The Hashemite Kingdom of Jordan.

[16] Wang, W., & Okaze, T. (2022). Statistical analysis of low-occurrence strong wind speeds at the pedestrian level around a simplified building based on the Weibull distribution. Building and Environment, 209, 108644. https://doi.org/10.1016/j.buildenv.2021.108644.

[17] Mithun Mondal, Djamal Hissein Didane, Alhadj Hisseine Issaka Ali, & Bukhari Manshoor. (2022). Wind Energy Assessment as a Source of Power Generation in Bangladesh. Journal of Advanced Research in Applied Sciences and Engineering Technology, 26(3), 16–22. https://doi.org/10.37934/araset.26.3.1622.

[18] Abdul Rashid Shoib, Djamal Hissein Didane, Akmal Nizam Mohammed, Kamil Abdullah, & Mas Fawzi Mohd Ali. (2021). Technical Assessment of Wind Energy Potentiality in Malaysia Using Weibull Distribution Function. Journal of Advanced Research in Fluid Mechanics and Thermal Sciences, 86(1), 1–13. https://doi.org/10.37934/arfmts.86.1.113.

[19] Teimourian, H., Abubakar, M., Yildiz, M., & Teimourian, A. (2022). A Comparative Study on Wind Energy Assessment Distribution Models: A Case Study on Weibull Distribution. Energies, 15(15), 5684. https://doi.org/10.3390/en15155684.

[20] AlQdah, K. S., Alahmdi, R., Alansari, A., Almoghamisi, A., Abualkhair, M., & Awais, M. (2021). Potential of wind energy in Medina, Saudi Arabia based on Weibull distribution parameters. Wind Engineering, 45(6), 1652–1661. https://doi.org/10.1177/0309524X211027356.

[21] Hassane, A. I., Didane, D. H., Tahir, A. M., & Hauglustaine, J.-M. (2018). Wind and Solar Assessment in the Sahelian Zone of Chad. International Journal of Integrated Engineering, 10(8). https://doi.org/10.30880/ijie.2018.10.08.026.

[22] Alami, A. H., Tawalbeh, M., Zhang, D., Aokal, K., Elsherbiny, L., Yasser, Z., & Abdelghani, A. (2018). Linear angstrom model applied to weather data collected for the city of Sharjah. In 2018 5th International Conference on Renewable Energy: Generation and Applications (ICREGA) (pp. 150–153). IEEE. https://doi.org/10.1109/ICREGA.2018.8337583.

[23] Serban, A., Paraschiv, L. S., & Paraschiv, S. (2020). Assessment of wind energy potential based on Weibull and Rayleigh distribution models. Energy Reports, 6, 250–267. https://doi.org/10.1016/j.egyr.2020.08.048.

[24] Al-Mhairat, B., & Al-Quraan, A. (2022). Assessment of Wind Energy Resources in Jordan Using Different Optimization Techniques. Processes, 10(1), 105. https://doi.org/10.3390/pr10010105.

[25] Al-Ghriybah, M., Fadhli, Z., Hissein, D., & Mohd, S. (2019). Wind energy assessment for the capital city of Jordan, Amman. Journal of Applied Engineering Science, 17(3), 311–320. https://doi.org/10.5937/jaes17-20241.

[26] Mohanad Al-Ghriybah. (2022). Assessment of Wind Energy Potentiality at Ajloun, Jordan Using Weibull Distribution Function. Evergreen, 9(1), 10–16. https://doi.org/10.5109/4774211.

[27] Wang, Z., & Liu, W. (2021). Wind energy potential assessment based on wind speed, its direction and power data. Scientific Reports, 11(1), 16879. https://doi.org/10.1038/s41598-021-96376-7.

[28] Onay, A. E., Dokur, E., & Kurban, M. (2021). Performance Comparison of New Generation Parameter Estimation Methods for Weibull Distribution to Compute Wind Energy Density. Elektronika Ir Elektrotechnika, 27(5), 41–48. https://doi.org/10.5755/j02.eie.28919.

[29] Safari, M. A. M., Masseran, N., & Majid, M. H. A. (2022). Wind energy potential assessment using Weibull distribution with various numerical estimation methods: a case study in Mersing and Port Dickson, Malaysia. Theoretical and Applied Climatology, 148(3–4), 1085–1110. https://doi.org/10.1007/s00704-022-03990-0.

[30] Wan, J., Zheng, F., Luan, H., Tian, Y., Li, L., Ma, Z., … Li, Y. (2021). Assessment of wind energy resources in the urat area using optimized weibull distribution. Sustainable Energy Technologies and Assessments, 47, 101351. https://doi.org/10.1016/j.seta.2021.101351.

[31] Nwokolo, S. C., Amadi, S. O., Obiwulu, A. U., Ogbulezie, J. C., & Eyibio, E. E. (2022). Prediction of global solar radiation potential for sustainable and cleaner energy generation using improved Angstrom-Prescott and Gumbel probabilistic models. Cleaner Engineering and Technology, 6, 100416. https://doi.org/10.1016/j.clet.2022.100416.

[32] Salau, A. O., Shonkora, S. S., & Owoeye, V. A. (2021). Analysis of Solar Energy Potential Using Sunshine Based Model. In 2021 IEEE AFRICON (pp. 1–4). IEEE. https://doi.org/10.1109/AFRICON51333.2021.9570973.

[33] Almorox, J., Voyant, C., Bailek, N., Kuriqi, A., & Arnaldo, J. A. (2021). Total solar irradiance's effect on the performance of empirical models for estimating global solar radiation: An empirical-based review. Energy, 236, 121486. https://doi.org/10.1016/j.energy.2021.121486.

[34] Ahamed, M. S., Guo, H., & Tanino, K. (2022). Cloud cover-based models for estimation of global solar radiation: A review and case study. International Journal of Green Energy, 19(2), 175–189. https://doi.org/10.1080/15435075.2021.1941043.

Paper submitted: 01.09.2022.

Paper accepted: 26.09.2022.